

# Decellularized fetal collagen exhibits chondroinductive potential for bone marrow-derived mesenchymal stem cells by enhancing glycosaminoglycan production

Soosai M. Amirtham<sup>1\*</sup>, Ganesh Parasuraman<sup>2\*</sup>, Jeya Lisha J<sup>1</sup>, Deepak V. Francis<sup>3</sup>, Abel Livingston<sup>4</sup>, Grace Rebekah<sup>5</sup>, Solomon Sathishkumar<sup>1</sup>, Elizabeth Vinod<sup>1,2</sup>

<sup>1</sup> Department of Physiology, Christian Medical College, Vellore, India

<sup>2</sup> Centre for Stem Cell Research, (A unit of InStem, Bengaluru), Christian Medical College, Vellore, India

<sup>3</sup> Department of Anatomy, Christian Medical College, Vellore, India

<sup>4</sup> Department of Orthopaedics, Christian Medical College, Vellore, India

<sup>5</sup> Department of Biostatistics, Christian Medical College, Vellore, India

\* Equal contribution

## SUMMARY

Articular cartilage repair is challenging due to limited access to reparative cells and a lack of self-healing mechanisms. Bone marrow-derived mesenchymal stem cells (BM-MSCs) are a promising therapeutic option, but their tendency to form fibrocartilage during repair necessitates the optimization of culture conditions. To overcome this limitation, optimizing in-vitro culture conditions with biological coating using extracellular matrix-derived proteins has been efficient in mimicking in-vivo cellular behavior. Fetal cartilage, with abundant collagen, proteoglycans and glycosaminoglycans has emerged as a potential source for cartilage repair. No studies have so far evaluated the effect of fetal cartilage-derived collagen on BM-MSCs. This study aimed to evaluate the chondro-inductive potential of decellularized

collagen derived from fetal cartilage, which was used as a coating material for expansion of BM-MSCs.

The extraction of fetal collagen was performed from the tibiofemoral joint of a 36+4-week gestational age fetus. The freeze-dried collagen type II was reconstituted at a concentration of 10µg/ml and used to coat the culture flasks. Passage 3 BM-MSCs were divided into two groups: a) standard expansion medium (BM-MSCs) and b) collagen-coated plasticware (collagen-coated BM-MSCs). Growth kinetics, surface markers, gene expression, and differentiation potential were assessed. The decellularized collagen coating did not influence the growth kinetics, surface marker and gene expression of BM-MSCs. However, it positively influenced GAG accumulation and collagen type II deposition. Further studies utilizing

## Corresponding author:

Dr. Elizabeth Vinod. Associate Professor/Adjunct Scientist. Department of Physiology/ Centre for Stem Cell Research (A unit of inStem, Bangalore), Christian Medical College, Vellore, India. Phone: +91 9677651977. E-mail: elsyclarence@cmcvellore.ac.in - ORCID: 0000-0001-7340-8320

Submitted: June 5, 2023. Accepted: July 8, 2023

<https://doi.org/10.52083/KJJC3228>

in-vivo models are warranted to evaluate the potential of collagen-coated BM-MSCs and exploit their adjuvant effect on chondrogenesis.

**Key words:** Fetal cartilage – Extracellular matrix collagen – Collagen type II – Chondrogenesis – BM-MSCs – Glycosaminoglycans

## INTRODUCTION

Hyaline cartilage plays an integral role in the mobility and weight-bearing functions of the articular joint. Cartilage loss due to inflammation or trauma, compounded by its restricted intrinsic regenerative capacity, can lead to the progression of osteochondral defects and conditions such as osteoarthritis (Sophia Fox et al., 2009). The most common treatment strategies currently used include debridement, microfracture, and intra-articular injections of biological scaffolds such as hyaluronic acid or platelet rich plasma. Despite symptomatic relief and the proposed minimization of disease progression, these techniques do not provide sustained clinical benefits (Armiento et al., 2019). Therefore, cell-based therapies and tissue engineering have recently received considerable attention to facilitate cartilage regeneration with hyaline-like properties (Negoro et al., 2018).

Cell-based therapies using mesenchymal stem cells (MSCs) and chondrocytes have demonstrated promising results in clinical trials (Filardo et al., 2013; Zhang et al., 2019). Bone-marrow-derived mesenchymal stem cells (BM-MSCs), due to their ease of harvest and availability, proliferative potential, immunomodulatory and multilineage capabilities, have been the most commonly used MSCs. Despite functional improvements, MSCs display a predilection for a hypertrophic phenotype, resulting in fibrocartilage formation, thus a repair tissue with inferior biomechanical properties (Charlier et al., 2019; Mueller and Tuan, 2009). To circumvent this limitation, a crucial strategy involves the optimization of in-vitro cell culture conditions. One effective approach is the implementation of extracellular matrix-derived proteins as a biological coating, which has demon-

strated efficacy in enhancing the cellular phenotype to closely mimic in-vivo behavior (Kleinman et al., 1987).

Fetal cartilage is another significant source that has been studied for its potential use in cartilage repair, specifically in conditions such as osteoarthritis (OA) and other degenerative joint disorders (Krivoruchko et al., 2014). Collagen is the main protein component of fetal cartilage, making up approximately 60-80% of the cartilage's dry weight (Quintin et al., 2010). Its unique characteristics include a higher concentration of chondroprogenitor cells, which further differentiate into chondrocytes that play a vital role in producing and maintaining the extracellular matrix of the cartilage (Choi et al., 2016). Second, fetal cartilage has a high concentration of extracellular matrix molecules, such as proteoglycans and glycosaminoglycans, that are essential for maintaining the structural integrity and mechanical properties of cartilage tissue (Fuchs et al., 2002). These molecules are critical for repairing and rebuilding damaged cartilage tissue.

Extracellular matrix (ECM) materials can be obtained from either cell-derived matrices secreted during in vitro culture or native tissues, with tissue-specific ECM reported to promote cell proliferation and lineage-specific differentiation by retaining biophysical and biochemical cues within native tissues (Benders et al., 2013). Decellularized ECM (Quintin et al., 2010) derived from cartilage tissues have been extensively researched as biological scaffolds for cartilage engineering due to their inherent components, unique structure, and micromechanical properties, which create a niche-like nanostructured microenvironment that supports chondrogenesis - cell adhesion, proliferation, migration, and differentiation (Schwarz et al., 2012; Yang et al., 2010).

Armed with their inherent properties, decellularized scaffolds seeded with stem cells are gaining attention in both basic research and clinical studies and have the potential for translating into functional tissues. No studies have so far evaluated the effect of fetal cartilage-derived collagen on BM-MSCs. The current study aimed to evaluate the chondro-inductive potential of decellularized collagen derived from fetal cartilage when

applied as a coating material for the expansion of BM-MSCs, using growth kinetics, surface marker expression, gene expression, biochemical GAG content, and differentiation study analysis. Additionally, the influence of fetal collagen on the hypertrophic markers was evaluated.

## MATERIALS AND METHODS

### Approval and study design

The study was performed after approval of the Institution Review Board and Ethics Committee. Following written informed consent, bone marrow aspirates were obtained from the surgical site of patients requiring total knee replacement surgery for severe OA (grade 4 Kellgren-Lawrence

score). BM-MSCs were isolated from bone marrow aspirate, expanded to passage 3, and characterized using flow cytometry. After obtaining written informed consent from the parent the fetal cartilage sample was extracted from the tibiofemoral joint of a fetus at 36+4 weeks gestational age, following termination of pregnancy due to medical reasons associated with intrauterine death.

The fetal cartilage shavings were decellularized and lyophilized to obtain collagen, which was subsequently utilized to coat the culture flasks. The BM-MSCs at passage 3 were seeded onto flasks coated with collagen and uncoated flasks (control) at a loading density of 5000 cells/cm<sup>2</sup>. The cells were cultured until they reached sub-confluence. The harvested cells were then subjected

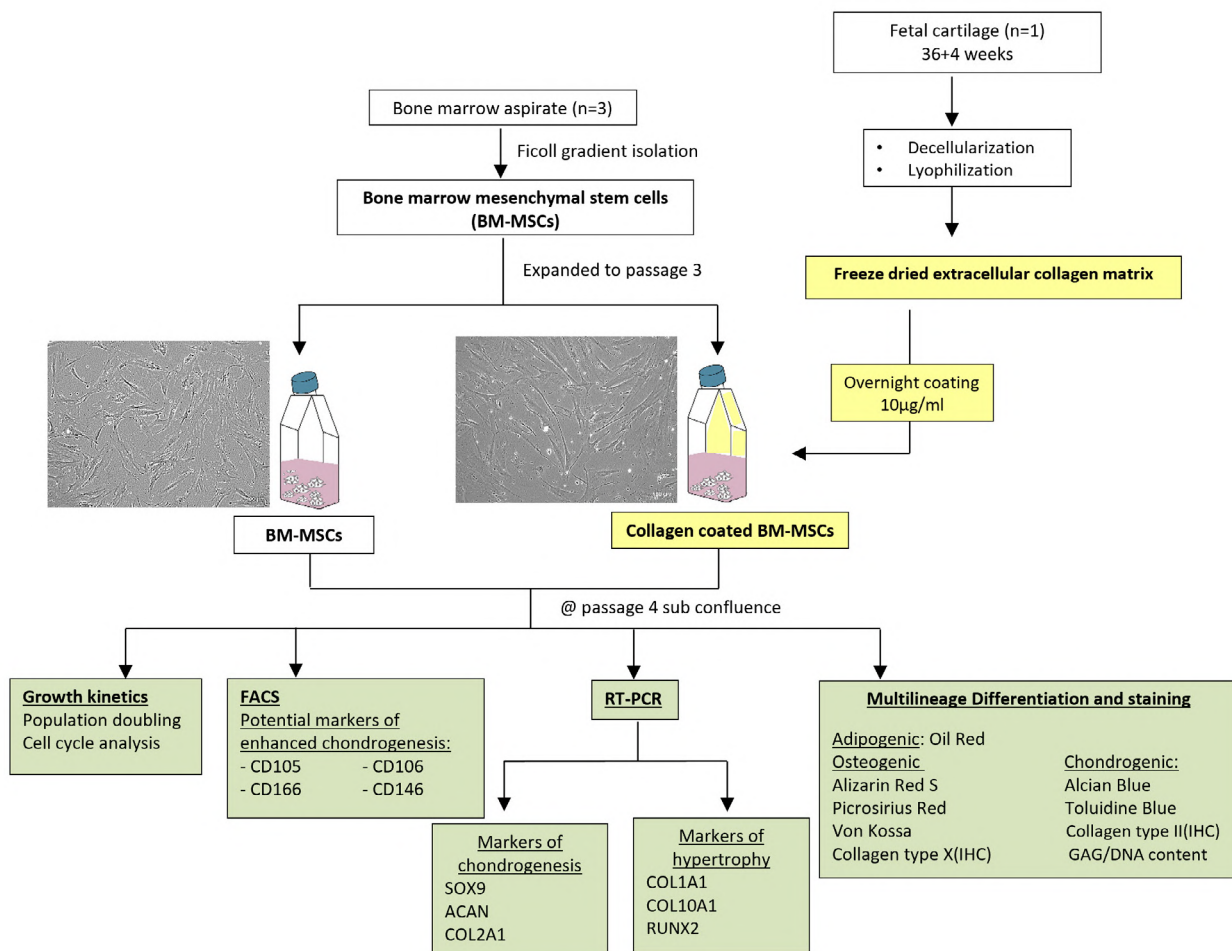


**Fig. 1.** - Study algorithm describing the evaluation parameters of bone marrow derived mesenchymal stem cells (BM-MSCs) grown under two culture conditions, namely the standard culture conditions (BM-MSC) and expansion on collagen coated plates (collagen coated BM-MSCs), which were derived from fetal cartilage. FACS: fluorescence activated cell sorting, CD: cluster of differentiation, SOX-9:(sex-determining region Y)-box 9, ACAN: aggrecan, COL: collagen, RUNX2: Runt-related transcription factor-2, IHC: immunohistochemistry and GAG: glycosaminoglycan.

to analysis based on the following parameters: a) growth kinetics, including population doubling and cell cycle analysis; b) FACS analysis for potential markers of chondrogenesis; c) quantitative real-time polymerase chain reaction (qRT-PCR) analysis to examine markers of chondrogenesis and hypertrophy; and d) trilineage differentiation, along with confirmatory staining (Fig. 1).

### Extraction and characterization of fetal collagen

The extraction of fetal collagen was performed using a modified protocol originally described by Feng et al. (2020). In brief, the tibio-femoral joint from the fetus was dissected and immediately placed in sterile phosphate-buffered saline solution (PBS). The joint was then transferred to a biosafety cabinet, washed in PBS and cleared of its external tissues. The cartilage was harvested and minced to 6-8 mm size using a 22-scalpel blade (Fig. 2A). A small portion of the section was formalin-fixed and subjected to DAPI (4',6-diamidino-2-phenylindole) staining to confirm the presence of nuclei before decellularization (Fig. 2D). The remaining cryo-sectioned cartilage was washed with PBS to remove the optimal cutting temperature (OCT) compound residue and im-

mersed at 25°C in 1% sodium dodecyl sulfate (SDS) for a period of 48 hours; this was followed by a wash with deionized water (Fig. 2B-E). This step was repeated three more times. DAPI staining was performed on the decellularized sheets for immunofluorescence analysis to confirm the absence of nuclei (Fig. 2F). The decellularized cartilage sections were transferred to a 100µM cell strainer and thoroughly washed to remove the SDS. The sections and the cell strainer were placed in a 6-well plate and pre-frozen overnight at -80°C. The following day, the tissue was transferred to a freeze-dryer and processed for lyophilization for 6 h (Fig. 2G). 10 mg freeze-dried extracellular matrix was further digested with pepsin (1mg/ml; Sigma) containing 0.01N HCl, using a shaking water bath maintained at 37°C for 72 h. The digest was neutralized with 0.01N NaOH to a pH of 7.4 and lyophilized again for 6 h. The freeze-dried vacuum end product was gamma irradiated at 10 gy, reconstituted with PBS, and used to coat the culture flasks at a final concentration of 10 µg/ml (overnight incubation at 4°C) (Fig. 2H). Western blot analysis using SDS-PAGE was performed to confirm the isolation of collagen type II (Fig. 2I).

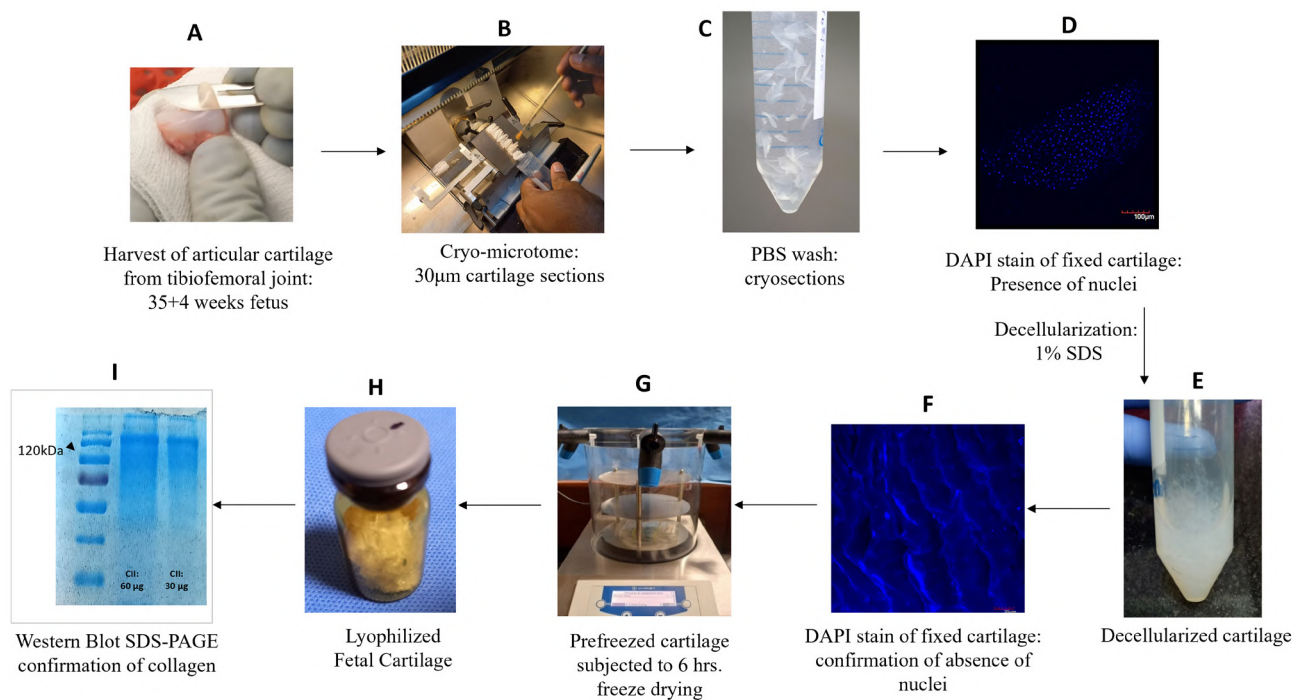


**Fig. 2.-** Flow algorithm illustrating the sequential steps involved in the isolation of freeze-dried extracellular collagen matrix from fetal cartilage.

### Isolation and culture of BM-MSCs

The bone marrow-derived aspirate was collected and transferred to vacutainers containing a pre-heparinized solution. Paque PREMIUM was added to the anticoagulated sample in the same proportion and gently mixed. Subsequently, the mixture was centrifuged at a force of 400 g for a duration of 45 minutes. The mononuclear cell layer obtained after two washes was loaded into T-75 flasks. After 24 hours, the non-adherent cells were washed with PBS and then replenished with a standard expansion medium. The expansion medium consisted of Alpha Eagle minimum essential medium containing 10% fetal bovine serum (FBS) and basic fibroblast growth factor 2 at a concentration of 1ng/mL. The adherent cells were cultured under standard conditions, maintaining 5% CO<sub>2</sub> at 37°C, until passage 3 for further experimentation. At passage 3 the BM-MSCs were loaded either on plain culture or collagen-coated culture flasks at a seeding density of 5000 cells/cm<sup>2</sup>. At sub-confluence, the cells were harvested and subjected for further analysis.

### Growth Kinetics: Cell cycle analysis, cell diameter and population doubling time

To determine the distribution of cells in different phases of the cell cycle, an analysis using DAPI (4',6-diamidino-2-phenylindole) was performed. The cells were trypsinized when they reached 60-70% confluence, and the analysis was conducted a day after changing the medium. The size of the cells was assessed using the CellDrop BF, DeNovix automated counter. Passage 4 BM-MSCs were washed with PBS and fixed for 1 hr with 70% cold ethanol. Following a wash, the cells were incubated with DAPI (1 µg/ml for 30 minutes using 0.1% TritonX-100) and subjected to flow cytometry analysis. The Flo-Jo software utilized the Watson algorithm to assess the proportion of cells in different phases during the analysis. To estimate the population doubling time (PDT) at passage 4 the following formulae were used:

$$PDT = \log 2 * \text{days in culture} / (\log (N1) - \log (No)),$$

N1: number of cells at confluence

No: initial number of cells seeded

### Fluorescence Activated Cell Sorting (FACS) for cell surface markers

The two cell groups were subjected to phenotypic analysis using the BD FACS CytoFLEX Flow Cytometer CytExpert. This analysis involved the inclusion of controls that were not stained with the antibody. The resulting data were then analyzed using BD FACS Diva v 8.0.1.1. Antibodies against the conjugated human surface antigens (BD-Bioscience) included: CD105-FITC, CD106-APC, CD166 BB515 and CD146-PE.

### qRT-PCR for gene expression

RNA was isolated from BM-MSCs and collagen-coated BM-MSCs using the Qiagen RNeasy Mini Kit. After determining the A260/A280 ratio and concentration using a Nanodrop Spectrophotometer, 280 ng of RNA was reverse-transcribed into cDNA using the Takara Bio First-Strand synthesis system. Quantitative real-time PCR (qRT-PCR) was performed using Takyon™ Low Rox SYBR Master Mix dTTP Blue (Eurogentec) with a final concentration of 7 ng of cDNA per reaction. The qRT-PCR was conducted using the Quantstudio 12K Flex thermocycler (Applied Biosystems). The gene profile analysis included SOX-9, ACAN, and COL2A1 for assessing chondrogenesis, as well as COL1A1, COL10A1, and RUNX2 to evaluate the hypertrophic expression profile. The relative mRNA expression for each gene was normalized to the reference housekeeping gene GAPDH ( $\Delta Ct$ ). The individual  $\Delta Ct$  values were compared to the collagen-coated BM-MSC group ( $\Delta \Delta Ct$ ), and the relative expression was calculated using the  $2^{-\Delta \Delta Ct}$  method. Table S1 provides a comprehensive list of detailed primer sequences, gene identifiers, accession codes, and base pair lengths.

### Trilineage differentiation and confirmatory staining

To induce differentiation into adipogenic, osteogenic, and chondrogenic lineages, Stem Pro differentiating kits from GIBCO were employed. For adipogenic differentiation, the cells were initially seeded at a density of 1000 cells/cm<sup>2</sup> and allowed to expand until reaching 80% confluence. Subsequently, the culture medium was replaced with adipogenic differentiation medium with me-

**Table S1.** Sequence of the primers used for RT-PCR. SOX9: sex determining region Y-box 9, ACAN: Aggrecan, COL2A1: Collagen type 2 alpha 1 chain, COL1A1: Collagen type 1 alpha 1 chain, COL10A1: Collagen type 10 alpha 1 chain, RUNX2: Runt related transcription factor-2 and MMP13: Matrix metalloproteinase type 13. GAPDH: glyceraldehyde 3-phosphate dehydrogenase.

Gene of Interest	Primers (5'-3')		Accession number (reference link)	Product size (bp)
	Forward primer	Reverse primer		
SOX-9	GACTTCCGCGACGTGGAC	GTTGGGCGGCAGGTAAGT	NM_000346.4 <a href="https://www.ncbi.nlm.nih.gov/nucleotide/1519242934">https://www.ncbi.nlm.nih.gov/nucleotide/1519242934</a>	99
ACAN, transcript variant 1	TCGAGGACAGCGAGGCC	TCGAGGGTGTAGCGTGTAGAGA	NM_001135.4 <a href="https://www.ncbi.nlm.nih.gov/nucleotide/1890265422">https://www.ncbi.nlm.nih.gov/nucleotide/1890265422</a>	85
COL2A1, transcript variant 2	CCTGAGTGGAAGAGTGGAGAC	TTGCTGCTCCACCAGTTCTT	NM_033150.3 <a href="https://www.ncbi.nlm.nih.gov/nucleotide/1674985896">https://www.ncbi.nlm.nih.gov/nucleotide/1674985896</a>	149
COL1A1	TCTGCGACAACGGCAAGGTG	GACGCCGGTGGTTTCTTGGT	NM_000088.4 <a href="https://www.ncbi.nlm.nih.gov/nucleotide/1777425449">https://www.ncbi.nlm.nih.gov/nucleotide/1777425449</a>	146
COL10A1	CAAGGCACCATCTCCAGGAA	AAAGGGTATTTGTGGCAGCATATT	NM_000493.4 <a href="https://www.ncbi.nlm.nih.gov/nucleotide/1519245829">https://www.ncbi.nlm.nih.gov/nucleotide/1519245829</a>	70
RUNX2, transcript variant 2	CCTAAATCACTGAGGCGGTC	CAGTAGATGGACCTCGGGAA	NM_001015051.4 <a href="https://www.ncbi.nlm.nih.gov/nucleotide/1890358904">https://www.ncbi.nlm.nih.gov/nucleotide/1890358904</a>	91
GAPDH transcript variant 7	TCAGCAATGCCTCCTGCAC	TCTGGGTGGCAGTGATGGC	NM_001357943.2 <a href="https://www.ncbi.nlm.nih.gov/nucleotide/1676440496">https://www.ncbi.nlm.nih.gov/nucleotide/1676440496</a>	117

dium change once in every three days for a period of three weeks. Oil Red O staining (0.5%) was performed following differentiation on the formalin fixed cells to confirm the accumulation of lipid vacuoles.

Osteogenic and chondrogenic differentiation was performed using a pellet culture system for a period of 28 days. In brief, one million cells were centrifuged at 400g for 12 min and left undisturbed for 48 hours to form a pellet. Following differentiation with respective differentiation medium, the pellets were washed and fixed with 4% paraformaldehyde, embedded in paraffin and sectioned. The 4 µm sections obtained were hydrated with descending grades of ethanol and subjected to their confirmatory staining.

To confirm the osteogenic staining, the pellets underwent staining with Alizarin Red S and Von Kossa. This was done to verify the presence of mineralized matrix accumulation. Additionally, Picrosirius red staining was used to determine the total collagen content, while immunohistochemical analysis was conducted to assess the presence of collagen type X. For the Von Kossa staining, the slides were immersed in a 1% silver

nitrate solution (Qualigens, Cat no: Q27462) and exposed to UV light in a chamber for 20 minutes. Subsequently, the excess silver nitrate was eliminated by treating it with a 5% sodium thiosulphate solution (Sigma, Cat no: 7772-98-7) for 5 minutes. Then, the samples were counterstained with nuclear fast red (ThermoFischer Scientific, Cat no: 211980050) for 5 minutes. Regarding the Alizarin Red staining (Sigma, Cat no: A5533), the slides were stained using a 2% Alizarin red solution (pH: 4.2, adjusted with ammonium hydroxide) for a duration of 5 minutes. PicroSirius Red (C.I.35782) staining was carried out utilizing a 0.1% concentration of the stain, followed by counterstaining with Hematoxylin. For immunohistochemistry, the paraffin sections were subjected to antigen retrieval using chondroitinase ABC (0.1 units/ml: 1 hour, C3667, Sigma Aldrich) and pepsin (pH 2.2, 1 mg/ml: 15 minutes, R2283, Sigma Aldrich). Following this, the sections were inhibited for endogenous peroxidase activity and subjected to protein block (6% FCS and 1% bovine serum albumin). Incubation with primary antibodies specific to collagen type X (1:200 dilution, 37°C) for 4 hours (ab49945, Abcam, Cambridge, UK) followed

by treatment with a secondary antibody, goat anti-mouse HRP-labeled immunoglobulin (31430, Pierce, Wisconsin, USA; 1:100 dilution) was performed. The final step involved staining with a chromogen solution containing 3,3-diaminobenzidine (DAB, Sigma, Cat no: D5637), followed by counterstaining with hematoxylin.

To confirm chondrogenic differentiation, the following protocol was employed for each stain: to assess the accumulation of glycosaminoglycans, the sections were treated with Alcian blue (pH: 2.5, Cat no: J60122, Alfa Aesar, US) for a duration of 5 minutes. Following this, the sections were counterstained with neutral red. In addition, Toluidine blue staining was conducted by incubating the sections in a 0.1% dye solution for 5 minutes (C.I. 52040 Qualigens).

To assess the Collagen type II content the paraffin sections were treated with pronase and hyaluronidase to retrieve them. The sections were then incubated with primary mouse monoclonal Anti-Collagen type II antibody (5 g/mL) (DSHB Hybridoma Product II-II6B3) at a temperature of 4°C overnight. This was followed by a 30-minute incubation with a secondary antibody at a dilution of 1:100, specifically HRP labeled goat anti-mouse immunoglobulin (31430, Pierce, Wisconsin, USA). Subsequently, the sections were stained with a 3,3-DAB for a duration of 5 minutes and counterstained with hematoxylin. After staining, all slides underwent dehydration and were cleared using xylene before being mounted with DPX for imaging.

### **Total GAG/DNA ratio**

The pellets following chondrogenic differentiation were subjected to digestion with papain solution containing cysteine, maintained at a temperature of 65°C for a duration of 16 hrs. Subsequently, quantitative analysis was performed to determine the content of glycosaminoglycans (GAG) and DNA. The concentration of DNA was measured using the Quant-iT Picogreen dsDNA reagent, with the standard curve generated using Lambda DNA. The fluorescence intensity (Ex  $\lambda$ : 480 nm, Em  $\lambda$ : 520 nm) was measured using a SpectraMax i3x Reader (Norwalk, CT, USA). The total GAG content was analyzed using the dimethyl methylene blue (DMMB) dye method, with

Chondrex, Inc Cat No: 6022 being utilized. Chondroitin 6-sulfate served as the standard for comparison. The optical density was measured using an Elisa plate reader at an absorbance of 525 nm. The resulting GAG values were then normalized to the DNA values, enabling the calculation of the total GAG/DNA ratio.

### **Statistical Analysis**

For data analysis, Microsoft Excel was used, while IGOR Pro Wave metrics Inc. (Version 5.0.4.8) was utilized for visual data presentation. The statistical analyses were performed using the Mann-Whitney U test for independent sample. In this study, the mean values along with the standard deviation or standard error of the mean were used to represent the data. P value less than 0.05 was considered significant.

## **RESULTS**

### **Growth Kinetics**

BM-MSCs displayed spindle shaped morphology in monolayer culture and expanded with similar morphological features up to passage 3. At passage 4, BM-MSCs cultured on collagen-coated plates displayed maintained fibroblastic appearance when compared to the control arm. Population Doubling Time (PDT) was assessed from cells at passage 4 subjected to the two different culture conditions. It was noted that both the groups showed similar PDT without any statistical difference between them (BM-MSC:  $5.25 \pm 0.11$  and collagen coated BM-MSC:  $4.61 \pm 0.21$ ). The examination of cell cycle distribution revealed that collagen coating did not significantly influence the growth kinetics of BM-MSCs during its expansion (Fig. 3A).

### **FACS for cell surface markers**

In comparing potential markers of enhanced chondrogenesis, both groups exhibited high expression levels of CD105 and CD166, as well as low expression of CD106, with no significant difference between them. However, when considering CD146, the collagen-coated BM-MSCs demonstrated a slightly higher average expression, although the difference was not statistically significant (Fig. 3B).

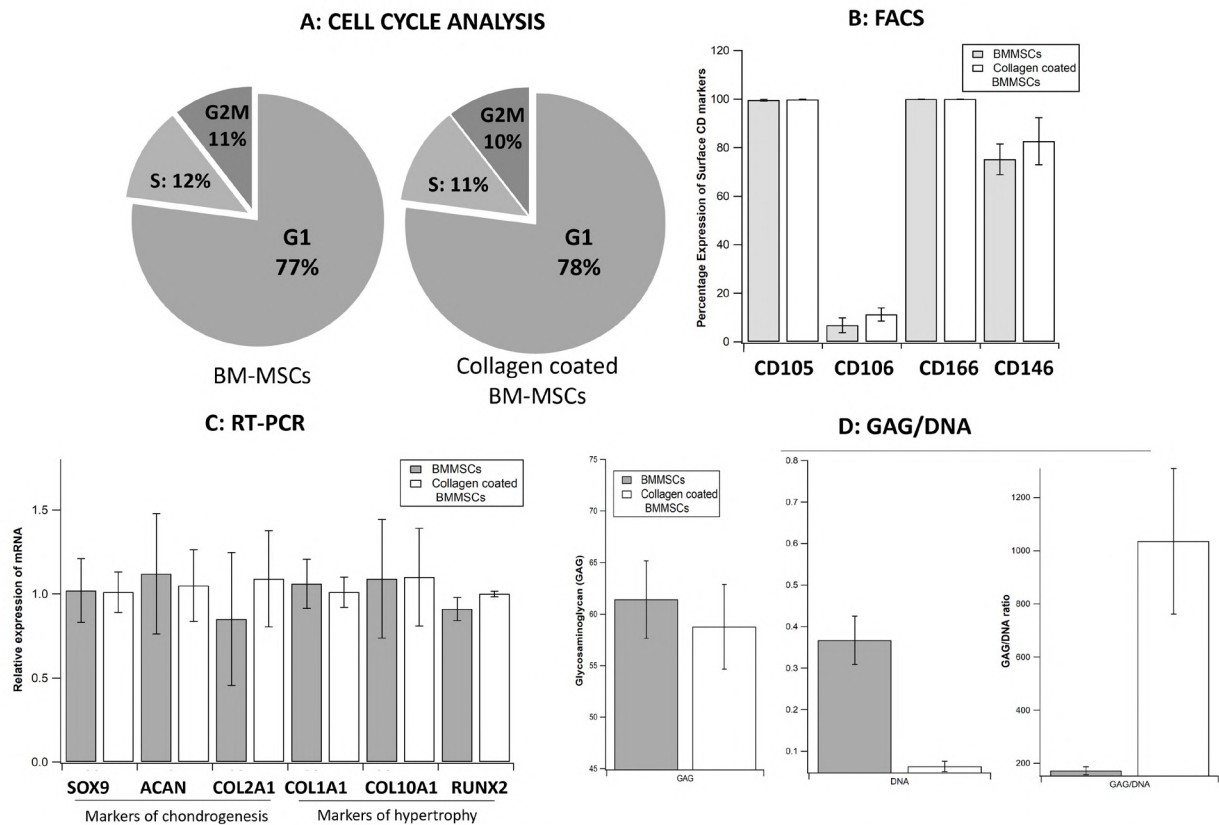


**Fig. 3.-** Comparative analysis between two groups of passage-4 BM-MSCs: the control group (BM-MSCs) and the collagen-coated BM-MSCs group. **A)** Percentage of cells in different phases of the cell cycle. **B)** Comparison of the percentage expression of cell surface markers associated with enhanced chondrogenesis. **C)** Comparison of the relative expression of SOX-9, ACAN, COL2A1, COL1A1, COL10A1, and RUNX2 among the two study groups.  $\Delta C_t$  indicates values that were normalized to GAPDH. To obtain the  $\Delta\Delta C_t$ , the individual  $\Delta C_t$  values were compared to the collagen-coated BM-MSC group, and the relative expression was calculated using the  $2^{-\Delta\Delta C_t}$  method. Data are presented as Mean  $\pm$  SD,  $n=3$ , with each sample performed in duplicates. SOX-9: (sex-determining region Y)-box 9, ACAN: aggrecan, COL2A1: collagen type 2A1, COL1A1: collagen type 1A1, COL10A1: collagen type 10A1, and RUNX2: Runt-related transcription factor-2. **D)** Quantitative estimation of GAG/DNA content in the chondrogenic differentiated pellet from the two groups. Values are expressed as Mean  $\pm$  SEM,  $n=3$ . GAG: glycosaminoglycans.

### qRT-PCR, trilineage differentiation and GAG/DNA

Comparable gene expression levels were observed in both groups, with high expression of SOX-9, ACAN, and COL1A1, and moderate expression of COL2A1, RUNX2, and COL10A1 (Fig. 3C). Both study groups demonstrated the ability for multilineage differentiation. Qualitative analysis of adipogenic differentiation showed similar uptake of Oil Red O by lipid droplets, while comparable uptake of Alizarin Red, Picrosirius Red, and Von Kossa stain indicated the deposition of calcified matrix (Fig. 4). Evaluation of pellets subjected to chondrogenic differentiation revealed improved staining with Alcian blue and Toluidine blue, as well as collagen type II deposition in the BMMSC collagen-coated pellets (Fig. 5). After digesting the chondrogenic-induced pellets and measuring the

DNA and GAG contents, it was observed that the BM-MSC collagen-coated group demonstrated markedly higher levels of GAG/DNA compared to the BM-MSC group. Specifically, the collagen-coated cells exhibited a substantial 4-11-fold increase in the total GAG/DNA ratio (Fig. 3D).

### DISCUSSION

Articular cartilage presents a compelling focus for tissue engineering due to the lack of direct access to a substantial supply of reparative cells and the absence of natural self-healing mechanisms following cartilage injuries (Sophia Fox et al., 2009). The utilization of BM-MSCs as a prominent cell-based therapeutic modality has garnered considerable attention due to their accessibility, abundant availability, notable proliferative potential, and immunomodulatory capacities (Zhang et

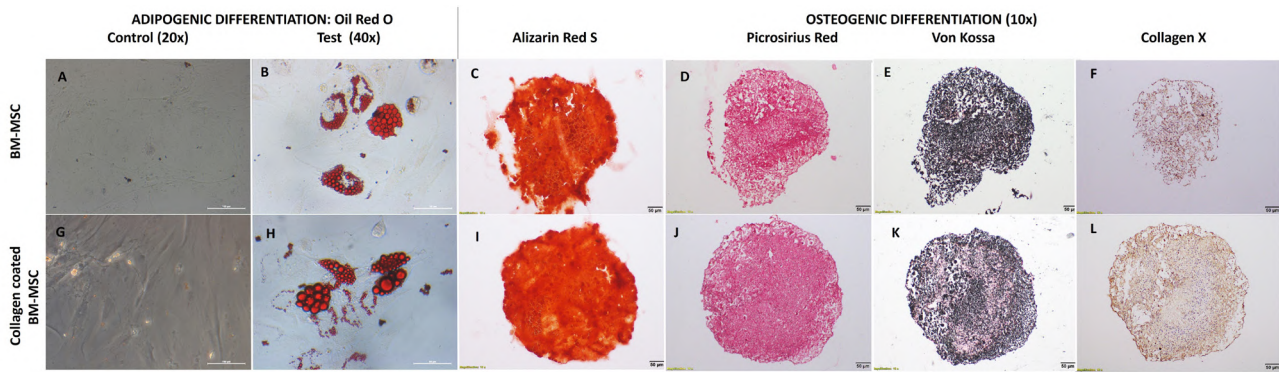


**Fig. 4.-** Adipogenic and osteogenic differentiation and staining of the two groups. Representative microscopic images of Oil Red O (A-B, G-H), Alizarin Red S (C, I), Picrosirius red (D, J), Von Kossa (E, K) and Collagen type X (F, L).

al., 2019). Nevertheless, researchers are increasingly directing their efforts towards optimizing in-vitro culture conditions to counteract the development of a hypertrophic phenotype and to enhance the quality of repair tissue generated by these cells. Fetal cartilage has been proposed as a promising source for cartilage repair because the extracellular matrix (ECM) contains high amounts of collagen II and glycosaminoglycan (GAG), similar to articular cartilage (Choi et al., 2016; Fuchs et al., 2002; Vinod et al., 2023). Fetal cartilage-derived cells have been successfully used in the treatment of arthritis (Krivoruchko et al., 2014). However, no studies have so far evaluated if collagen derived from fetal cartilage can be utilized for coating materials for refining the cellular behavior and phenotype of cells during culture. This study aimed to develop a collagen-based coating for BM-MSC expansion and assess whether the

microenvironment would enhance the chondrogenic ability of BM-MSCs.

In this study, collagen was successfully isolated from fetal cartilage, and its presence was confirmed by western blot analysis, revealing the presence of collagen type II. Culturing BM-MSCs on the collagen-coated surface did not impact their proliferative potential or morphological characteristics. CD106, a well-established marker for mesenchymal stem cells, has been recognized as a potential predictive marker for osteogenesis (Liu et al., 2008). Additionally, CD105, apart from its role as an MSC marker, has been documented as a predictive marker for chondrogenesis (Fan et al., 2016; Wang et al., 2013). Conversely, CD166 and CD146 are regarded as putative markers associated with improved chondrogenesis (Dicks et al., 2019; Vinod et al., 2021; Wu et al., 2016). It was noted that the expansion of BM-MSCs on collagen

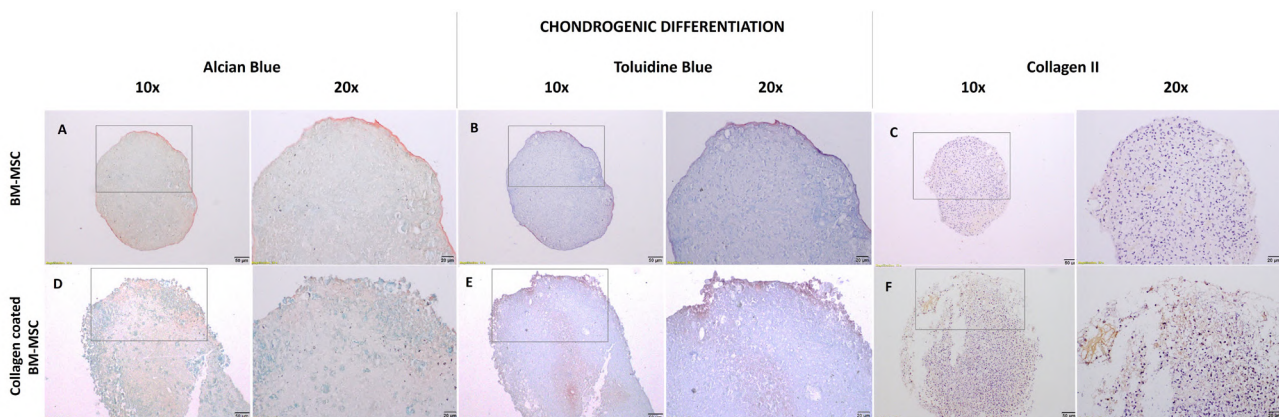


**Fig. 5.-** Chondrogenic differentiation and staining of the two groups. Representative microscopic images of Alcian blue (A, D), Toluidine blue (B, E) to assess uptake of glycosaminoglycans and Collagen type II (C, F).

coating did not influence their surface marker profile, as no significant difference was observed when comparing the putative markers of chondrogenesis with the group grown under standard conditions. A comparison between BM-MSCs and collagen-coated BM-MSCs revealed that the latter exhibited higher levels of collagen type II, which aligned with the staining observed in the immunohistochemical analysis. In terms of GAG/DNA analysis, collagen coating positively influenced BM-MSCs, resulting in a seven-fold increase in GAG accumulation with the differentiated pellets demonstrating improved uptake of Alcian blue and toluidine blue.

This study represents the first in-vitro investigation to utilize collagen derived from fetal cartilage and examine its influence on BM-MSCs. Although not statistically significant, it is noteworthy that fetal collagen coated BM-MSCs demonstrated an increase in GAG accumulation. Another significant finding was that, despite the presence of mineralization following osteogenic differentiation with collagen-coated BM-MSCs, there were no changes observed in their hypertrophy gene expression. Further studies utilizing in-vivo models are warranted to evaluate the potential of collagen-coated BM-MSCs and exploit their adjuvant effect on chondrogenesis.

## ACKNOWLEDGEMENTS

SMA and EV were involved in the study's conception and design. SMA, GP, JLJ, DVF, AL and EV performed the experiments and collected data. All authors were involved in data analysis and interpretation. EV and SMA provided financial support. All authors were involved in preparing the final version of the manuscript. We acknowledge Ms. Sevanthy Suresh, Mr. Abdul Muthallib, Ms. Esther Rani and Mr. Ashok Kumar for technical support, and the Centre for Stem Cell Research (A unit of inStem Bengaluru), Christian Medical College, Vellore for infrastructural support. This project was supported by the Fluid Research Grant (IRB Min No: 14498 dated 23.02.2022), Christian Medical College, Vellore.

## REFERENCES

ARMIENTO AR, ALINI M, STODDART MJ (2019) Articular fibrocartilage—Why does hyaline cartilage fail to repair? *Adv Drug Delivery Rev*, 146: 289-305.

BENDERS KEM, VAN WEEREN PR, BADYLAK SF, SARIS DBF, DHERT WJA, MALDA J (2013) Extracellular matrix scaffolds for cartilage and bone regeneration. *Trends Biotechnol*, 31(3): 169-176.

CHARLIER E, DEROYER C, CIREGIA F, MALAISE O, NEUVILLE S, PLENER Z, MALAISE M, DE SENY D (2019) Chondrocyte dedifferentiation and osteoarthritis (OA). *Biochem Pharmacol*, 165: 49-65.

CHOI WH, KIM HR, LEE SJ, JEONG N, PARK SR, CHOI BH, MIN B-H (2016) Fetal cartilage-derived cells have stem cell properties and are a highly potent cell source for cartilage regeneration. *Cell Transplant*, 25(3): 449-461.

DICKS A, WU C-L, STEWARD N, ADKAR SS, GERSBACH CA, GUILAK F (2019) Prospective Isolation of chondroprogenitors from human iPSCs based on cell surface markers identified using a CRISPR-Cas9-generated reporter. *BioRxiv*, 675983.

FAN W, LI J, WANG Y, PAN J, LI S, ZHU L, GUO C, YAN Z (2016) CD105 promotes chondrogenesis of synovium-derived mesenchymal stem cells through Smad2 signaling. *Biochem Biophys Res Commun*, 474(2): 338-344.

FENG B, JI T, WANG X, FU W, YE L, ZHANG H, LI F (2020) Engineering cartilage tissue based on cartilage-derived extracellular matrix cECM/PCL hybrid nanofibrous scaffold. *Materials Design*, 193: 108773.

FILARDO G, MADRY H, JELIC M, ROFFI A, CUCCHIARINI M, KON E (2013) Mesenchymal stem cells for the treatment of cartilage lesions: From preclinical findings to clinical application in orthopaedics. *Knee Surg Sports Traumatol Arthrosc*, 21(8): 1717-1729.

FUCHS JR, TERADA S, HANNOUCHE D, OCHOA ER, VACANTI JP, FAUZA DO (2002) Engineered fetal cartilage: Structural and functional analysis in vitro. *J Pediatr Surg*, 37(12): 1720-1725.

KLEINMAN HK, LUCKENBILL-EDDS L, CANNON FW, SEPHEL GC (1987) Use of extracellular matrix components for cell culture. *Analytical Biochem*, 166(1): 1-13.

KRIVORUCHKO N, TUGANBEKOVA S, RAKHIMBEKOVA G, KUZEMBAEVA K, ZARIPOVA L (2014) The results of fetal chondrocytes transplantation in patients with rheumatoid arthritis. *Central Asian J Global Health*, 3(Suppl), 164.

LIU F, AKIYAMA Y, TAI S, MARUYAMA K, KAWAGUCHI Y, MURAMATSU K, YAMAGUCHI K (2008) Changes in the expression of CD106, osteogenic genes, and transcription factors involved in the osteogenic differentiation of human bone marrow mesenchymal stem cells. *J Bone Mineral Metab*, 26(4): 312-320.

MUELLER MB, TUAN RS (2008) Functional characterization of hypertrophy in chondrogenesis of human mesenchymal stem cells. *Arthritis Rheum*, 58(5): 1377-1388.

NEGORO T, TAKAGAKI Y, OKURA H, MATSUYAMA A (2018) Trends in clinical trials for articular cartilage repair by cell therapy. *NPJ Regen Med*, 3: 17.

QUINTIN A, SCHIZAS C, SCALETTA C, JACCOUD S, APPLIGATE LA, PIOLETTI DP (2010) Plasticity of fetal cartilaginous cells. *Cell Transplant*, 19(10): 1349-1357.

SCHULZE-TANZIL G (2009) Activation and dedifferentiation of chondrocytes: Implications in cartilage injury and repair. *Ann Anat*, 191(4): 325-338.

SCHWARZ S, KOERBER L, ELSAESSER AF, GOLDBERG-BOCKHORN E, SEITZ AM, DÜRSELEN L, IGNATIUS A, WALTHER P, BREITER R, ROTTER N (2012) Decellularized cartilage matrix as a novel biomatrix for cartilage tissue-engineering applications. *Tissue Eng. Part A*, 18(21-22): 2195-2209.

SOPHIA FOX AJ, BEDI A, RODEO SA (2009) The basic science of articular cartilage. *Sports Health*, 1(6): 461-468.

VINOD E, PADMAJA K, LIVINGSTON A, JAMES JV, AMIRTHAM SM, SATHISHKUMAR S, RAMASAMY B, REBEKAH G, DANIEL AJ, KACHROO U (2021) Prospective isolation and characterization of chondroprogenitors from human chondrocytes based on CD166/CD34/CD146 surface markers. *Cartilage*, 13(2 suppl): 808S-817S.

VINOD E, PARASURAMAN G, LISHA JJ, AMIRTHAM SM, LIVINGSTON A, VARGHESE JJ, RANI S, VINOD FRANCIS D, REBEKAH G, DANIEL AJ, RAMASAMY B, SATHISHKUMAR S (2023) Human fetal cartilage-derived chondrocytes and chondroprogenitors display a greater commitment to chondrogenesis than adult cartilage resident cells. *PLoS One*, 18(4): e0285106.

WANG M, CHEN P, LIU C, HAO Y, ZHANG Y, ZHANG X (2013) Experimental study on CD105+/CD166+ cells and its chondrogenic potential in early osteoarthritis cartilage. *Zhongguo Xiu Fu Chong Jian Wai Ke Za Zhi = Chinese J Rep Reconstr Surg*, 27(7): 793-799.

WU C-C, LIU F-L, SYTWU H-K, TSAI C-Y, CHANG D-M (2016) CD146+ mesenchymal stem cells display greater therapeutic potential than CD146- cells for treating collagen-induced arthritis in mice. *Stem Cell Res Therapy*, 7: 23.

YANG Z, SHI Y, WEI X, HE J, YANG S, DICKSON G, TANG J, XIANG J, SONG C, LI G (2010) Fabrication and repair of cartilage defects with a novel acellular cartilage matrix scaffold. *Tissue Eng Part C Methods*, 16(5): 865-876.

ZHANG R, MA J, HAN J, ZHANG W, MA J (2019) Mesenchymal stem cell related therapies for cartilage lesions and osteoarthritis. *Am J Translat Res*, 11(10): 6275-6289.